



HAL
open science

Revisiting diesel fuel formulation from Petroleum light and middle refinery streams based on optimized engine behavior

Arij Ben Amara, Roland Dauphin, Hassan Babiker, Yoann Viollet, Junseok Chang, Nicolas Jeuland, Amer Amer

► To cite this version:

Arij Ben Amara, Roland Dauphin, Hassan Babiker, Yoann Viollet, Junseok Chang, et al.. Revisiting diesel fuel formulation from Petroleum light and middle refinery streams based on optimized engine behavior. *Fuel*, 2016, 174, pp.63-75. 10.1016/j.fuel.2016.01.062 . hal-01293384

HAL Id: hal-01293384

<https://hal.science/hal-01293384>

Submitted on 24 Mar 2016

HAL is a multi-disciplinary open access archive for the deposit and dissemination of scientific research documents, whether they are published or not. The documents may come from teaching and research institutions in France or abroad, or from public or private research centers.

L'archive ouverte pluridisciplinaire **HAL**, est destinée au dépôt et à la diffusion de documents scientifiques de niveau recherche, publiés ou non, émanant des établissements d'enseignement et de recherche français ou étrangers, des laboratoires publics ou privés.

1 Revisiting diesel fuel formulation from Petroleum light and middle 2 refinery streams based on optimized engine behavior

3 *Arij Ben Amara*¹, *Roland Dauphin*¹, *Hassan Babiker*², *Yoann Viollet*², *Junseok Chang*², *Nicolas*
4 *Jeuland*^{1,3}, *Amer Amer*²

5 ¹ IFP Energies Nouvelles, 1-4 avenue de Bois-Préau 92852 Rueil-Malmaison Cedex, France

6 ² Saudi Aramco, R&D Center, PO Box 62, Dhahran 31311, Saudi Arabia

7 ³ Present address: Safran Tech, Paris-Saclay, France

8 * Corresponding author

9 Contact: arij.ben-amara@ifpen.fr

10 Abstract

11 The share of diesel fuel in European transport sector, which currently represents over 50% of total
12 demand, is increasing, requiring massive imports of this product, while at the same time, gasoline fuels are
13 today in surplus. In terms of air pollutant emissions, gasoline and kerosene streams have shown potential
14 in achieving lower emissions in Compression Ignition (CI) engines, particularly nitrogen oxides (NO_x)
15 and particulates. A new fuel formulation approach through the use of light fractions within diesel
16 technology could consequently address both questions of energy demand balance and reduction of diesel
17 engines pollution footprint. In this study, a fuel formulation for a Diesel engine is optimized to achieve
18 lower pollutants emissions and higher engine efficiency. The fuel matrix is based on seven refinery
19 streams representative of gasoline (Hydrotreated Straight-Run Gasoline HSRG, Hydrotreated Fluid
20 Catalytic Cracking HFCC and Reformate REF), kerosene (Hydrotreated Straight-Run Kerosene HSRK
21 and Hydrocracked Kerosene HCKK) and diesel cuts (Hydrotreated Straight-Run Diesel HSRD and
22 Hydrocracked Light Diesel HCKLD). A D-Optimal mixture design is applied to build, a 12-run, 7-factor

23 fuel matrix and the fuels are thoroughly optimized on two engine conditions at light and mid-load
24 representative of typical vehicle running conditions. The results show a high sensitivity and a good
25 correlation of the engine efficiency and pollutants emissions with the volumetric contribution of each
26 refinery stream to the fuel composition. The optimum fuel composition varies across the range of engine
27 operating points. At light load for example, the addition of up to 50%v of gasoline streams (HSRG and
28 HFCC) to diesel streams demonstrates a good potential to simultaneously reduce NO_x and particulate
29 emissions and an overall good engine performance. Reformate, a highly aromatic gasoline stream, did not
30 offer an advantage at any of the tested conditions due to high particulate emissions. The two kerosene
31 streams perform similarly to diesel streams in terms of engine efficiency and pollutants emissions. A
32 compromise fuel, composed of 50%v HSRG and 50%v HSRD, is proposed that allowed halving NO_x and
33 particulate emissions and reducing the fuel consumption by 5%wt compared to reference diesel HSRD.
34 The optimized fuel represents an alternative for balancing diesel and gasoline demand and for pollutant
35 emissions reduction.

36 ***Keywords***

37 Naphtha, Straight-Run Gasoline, Design of Experiment DoE, formulation, optimization, pollutants,
38 efficiency, NO_x, particulates.

39

40

41

42

43

44 **1 Introduction**

45 Energy and environmental concerns are driving several changes in the European transport sector, with
46 increasing incentives towards alternative renewable energy sources and new refining processes. However,
47 conventional fossil fuels remain the sector's major energy source. Conventional liquid fuels represented
48 95% of European demand in 2012 [1] and according to recent forecasts from the European Commission,
49 are likely to remain dominant over the coming decades [2]. For transport applications, the share of diesel
50 fuel represents over 50% of the European market (in comparison with gasoline and jet fuel, 32% and 14%
51 respectively) and demand is rising [2]. The main drivers for such high demand are the high efficiency of
52 diesel engines and recent improvements of after-treatment systems, noise and drivability. Conversely,
53 light products like gasoline cuts, issuing from straight run distillation or Fluid Catalytic Cracking (FCC), a
54 conversion process widely used in European refineries, are today in surplus. This has drawn much
55 attention to their use as an alternative fuel in diesel engines to balance the energy demand and to meet
56 future pollutant emissions legislation. To achieve pollutant targets for light duty diesel engines, several
57 technological solutions are used to enhance the control of ignition timing and combustion rate [3]
58 including variable compression ratio, adapted injection systems, improved piston geometry, increased
59 exhaust gas recirculation (EGR) rates, and improved cooling or boosting capacity [4],[5],[6],[7]. However,
60 the physical and chemical characteristics of a fuel can have an important impact on mixture formation,
61 ignition and heat release rate [8],[9]. Higher volatility enhances the mixture formation during the ignition
62 delay and a lower cetane number delays the ignition occurrence, mainly at low-to-mid loads [10].
63 Increasing fuel volatility in fuels of similar chemical composition has shown a soot reduction potential in
64 CI engines for diesel and kerosene cuts due to the reduction of over-rich areas, and a moderate effect for
65 gasoline cuts [11]. Increasing diesel volatility at equal cetane number [12] leads to a reduction of liquid
66 film formation on cylinder walls, and thus, a reduction in smoke and enhanced fuel-conversion efficiency.
67 The application of highly mixed combustion modes however presents the disadvantage of a load range
68 limited by difficult combustion control at high load and an increase in HC and CO due to lower

69 combustion efficiency [7]. Fuel wall impingement, the crevices, boundary layers, and fuel-lean regions
70 formed during longer auto-ignition delay may constitute additional sources of HC and CO emissions [13],
71 [14], [15].

72 **Petroleum-based formulations for Diesel engines and impacts on pollutants**

73 The use of gasoline or kerosene as alternatives to diesel fuel has been studied by several groups for their
74 pollutants reducing potential. Han et al. [16] proved a simultaneous reduction of NO_x and soot emissions
75 using up to 40% gasoline with low EGR requirement compared to diesel fuel. CO and HC emissions were
76 comparable to diesel engines at light loads, however increased at high loads [17]. Kerosene fuels are also
77 attractive for their higher volatility and lower cetane number, generally between EU diesel and gasoline.
78 Tested alone in compression ignition engines, kerosene presents lower NO_x emissions than diesel at a
79 similar soot level [18] [19] and in mixture with diesel, it enhances the combustion efficiency [20]. The
80 chemical effect of fuel formulation is difficult to separate from the physical effect, especially in complex
81 engine configurations. Nevertheless, several general trends have been put forward in recent literature.
82 Most usually, fuels containing high level of aromatics increase soot formation [10] [21]. Diminishing the
83 aromatic content generally correlates with particulate reduction for diesel, gasoline and kerosene
84 distillation cuts [11]. Paraffinic saturated fuels have, in comparison, lower soot tendency regardless of
85 their molecular structure [22] [23]. Note however, the exception of fuels containing a high proportion of
86 long-chain normal paraffins, which may lead to enhanced soot formation through increasing fuel
87 ignitability and the creation of local rich areas [21]. Unsaturated hydrocarbons, namely, monoaromatics
88 and short-chain olefins, can lead to over 2 and 5 folds higher NO_x tendency respectively when compared
89 to paraffinic saturated compounds [24]. Aromatic-rich fuels can have longer ignition delay times but can
90 also form higher level of NO_x towards the end of the combustion [25]. The safety question related to
91 lighter fractions introduction in Diesel fuels has been recently addressed by Al-Abdullah et al. [26] where
92 the flash points (FP) and volatilities of blends of a commercial diesel and a commercial gasoline were
93 measured. According to their results, the flash point decreases as the concentration of gasoline is

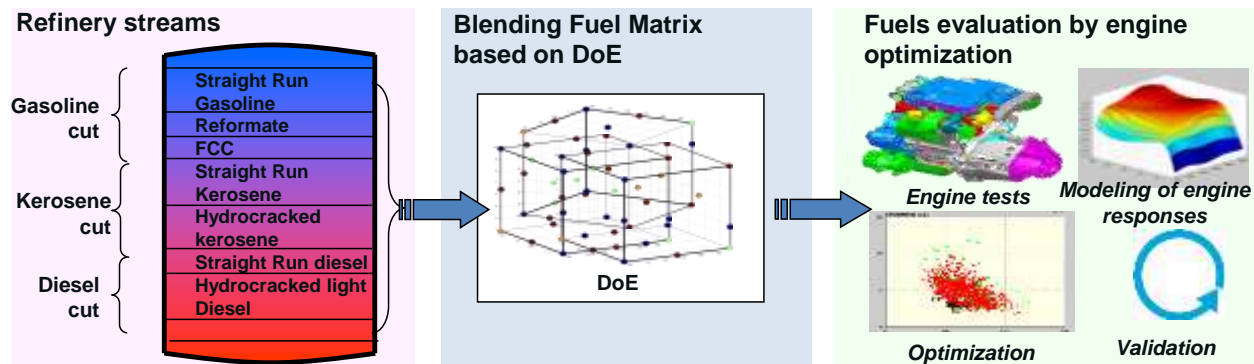
94 increased. For a mixture of 16%vol of gasoline in diesel, FP reaches 40°C. These results suggest that
95 blends with high gasoline fractions should present very similar behavior compared with gasoline which
96 has a FP of 45°C.

97 **Modeling approaches for fuel design**

98 Optimizing a fuel's formulation for advanced combustion modes requires an accurate knowledge of the
99 fuel's behavior over a wide range of engine operating conditions, both in steady state and transient modes.
100 To better address these complex physical and chemical phenomena involved, statistical modeling
101 approaches can represent powerful tools. Especially, Design of Experiments (DoE), refers to the process
102 of planning, designing and analyzing the experiments. It involves the development of statistical relations
103 between the response variables and the input factors and their interactions. In engine applications, DoE
104 have been widely applied in engine optimization processes [27]. DoE has also been used to optimize fuel
105 properties in terms of cetane number (CN), volatility and total aromatics content [28]. However, to our
106 knowledge, few studies have used DoE to optimize the fuel formulation with regards to combustion
107 behavior. In this study, we propose to evaluate a DoE approach to optimize fuel formulation for diesel
108 engines based on existing refinery streams, to improve engine efficiency and reduce main pollutant
109 emissions. Engine outputs were modeled as a function of the fuel composition and an optimum fuel is
110 proposed.

111 **2. Materials and methods**

112 Figure 1 presents the layout of the present study: first, seven refinery streams used in road and air
113 transport were selected. A 12-run, 7-factor D-Optimal mixture design was then generated using Design-
114 Expert® version 9. The seven refinery streams constitute the design variables while engine outputs
115 correspond to the response parameters. Engine outputs were then modeled by first order models with
116 regards to the volume fraction of the streams and the models presenting good quality were used to
117 determine an optimum fuel composition.



118

119

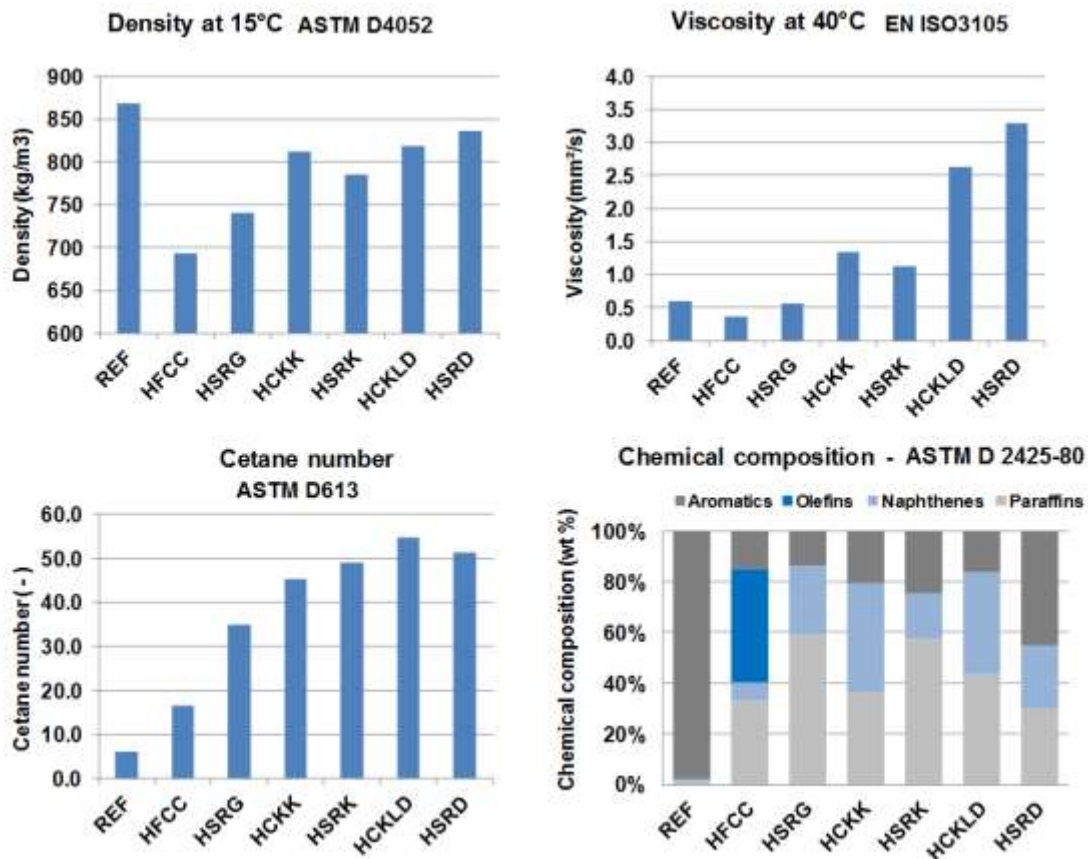
Figure 1: Scheme of the study outline

120 2.1 Refinery streams

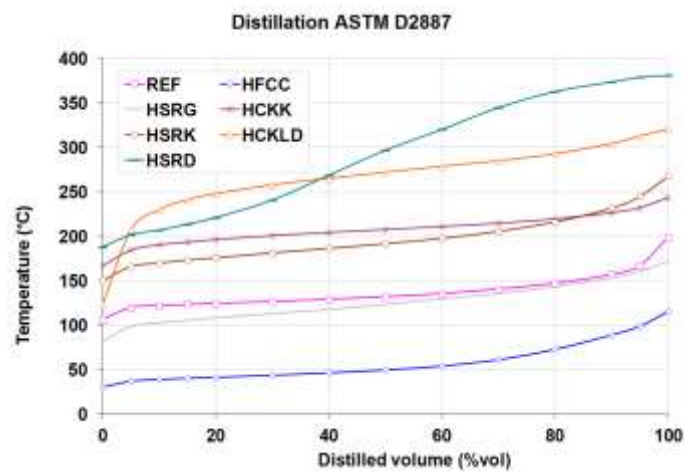
121 Seven refinery streams representative of gasoline, kerosene and diesel cuts were selected involving three
 122 straight-run streams: Hydrotreated Straight Run Gasoline, Kerosene and Diesel, noted, HSRG, HSRK,
 123 HSRD, respectively. Main streams properties are presented in Figure 2. Hydrocracked kerosene (HCKK)
 124 and light diesel (HCKLD), Hydrotreated Fluid Catalytic Cracking (HFCC) chosen for its high olefins
 125 content (near 45%wt) and reformate (REF) constituted of over 97%wt aromatics were selected as the
 126 remaining four streams. REF and HSRD were supplied by Coryton Advanced Fuels, and the remaining
 127 streams were provided by various Saudi Arabian refineries. All streams have a sulfur content below 10
 128 ppm, except for HSRK which contains 220 ppm (the detailed composition of sulfur containing species
 129 were not determined during this work), and they cover a broad distillation range from 35°C to 380°C.
 130 Initial Boiling Points vary from 35°C to 188°C and Final Points from 115°C to 380°C. Stream densities
 131 vary from 692 to 868 kg/m³ and kinematic viscosity from 0.36 to 3.3mm²/s. Gasoline and kerosene
 132 streams have lower values of density and viscosity compared to diesel streams. Paraffins-Olefins-
 133 Naphthenes-Aromatics (PONA) composition was determined by gas chromatography mass spectrometry
 134 GC-MS analysis and the most paraffinic fuels are the HSRG and HSRK, while naphthenes are the highest
 135 in hydrocracked streams (up to 40%wt). REF is composed of over 97%wt aromatics mainly branched
 136 monoaromatics (toluene and xylenes), followed by HSRD (45%wt) which has the highest yield of
 137 polyaromatics (3.6%wt). Olefins are present exclusively in HFCC at 45%wt. The cetane number was

138 assessed by CFR technique except for REF and HFCC whose cetane was evaluated by a blending method.

139 The CN of the streams ranges from 6 to 55. Detailed analysis of the streams is provided in Appendix A.



140



141

142

Figure 2: Main fuel properties of the seven selected refinery streams

143 **2.2 Fuel matrix definition by Design of Experiment approach**

144 To optimize fuel composition, a 12-run, 7-factor D-Optimal mixture design was generated using Design-
145 Expert® version 9 [29]. The seven refinery streams constituted the design variables while the engine
146 outputs corresponded to the response parameters. Statistical first-order linear models with no interaction
147 were defined and the matrix was built under constraints of the domain limits. Those limits consisted of the
148 range of cetane number, fractions of diesel, gasoline and kerosene cuts and maximum total aromatics.
149 Hence, the CN range was defined from 35 to 51 (+/-2). The upper limit corresponds to current European
150 diesel specification, and the lower was set to reduce the risk of combustion instability at light load based
151 on previous studies from our group [5]. The proportion of gasoline and kerosene streams was allowed up
152 to 50%vol for each [11] [17] [16] [30], and a minimum of 30%vol of diesel streams was required to allow
153 for high load performance and a sufficient viscosity [5]. In addition, total aromatic content was capped at
154 50% to limit smoke emissions. The matrix design was composed of 12 (Fuels 1-12) ranked in order of
155 decreasing cetane number. These fuels included a reference diesel fuel (Fuel 4), binary blends of
156 diesel/kerosene streams (Fuel 1 and 2), binary blends of diesel/gasoline streams: Fuels 3 and 12 containing
157 7%vol and 41%vol Reformate, Fuels 5 and 6 containing 50%vol HSRG and Fuels 10-11 containing 50%
158 HFCC. Two ternary blends of diesel/kerosene/gasoline streams (Fuels 8-9) and a central point (Fuel 7)
159 composed of all tested streams was set as repeatability point and tested 8 times throughout the study
160 (Table 1). Finally, a validation fuel was also formulated (Fuel 13) composed of 50%HCKK, 30%HSRD
161 and 20%HSRG. The matrix is detailed in Table 1. The fuels' properties cover a wide range of physical
162 and chemical properties, some of which were outside the limits of European diesel fuel specifications
163 EN590, especially in terms of density and viscosity. The fuels were treated with lubricity additive
164 (OLI9000 from Innospec) and antioxidant additive (Butylated HydroxyToluene - BHT) to ensure
165 mechanical component durability and a consistent fuel quality throughout the study.

166

167 *Table 1: Fuel matrix: Fuel 1-12, Fuel 7 corresponds to the central fuel and was tested 8 times throughout*
 168 *the study, Fuel 13 is the validation fuel (used for models validation)*

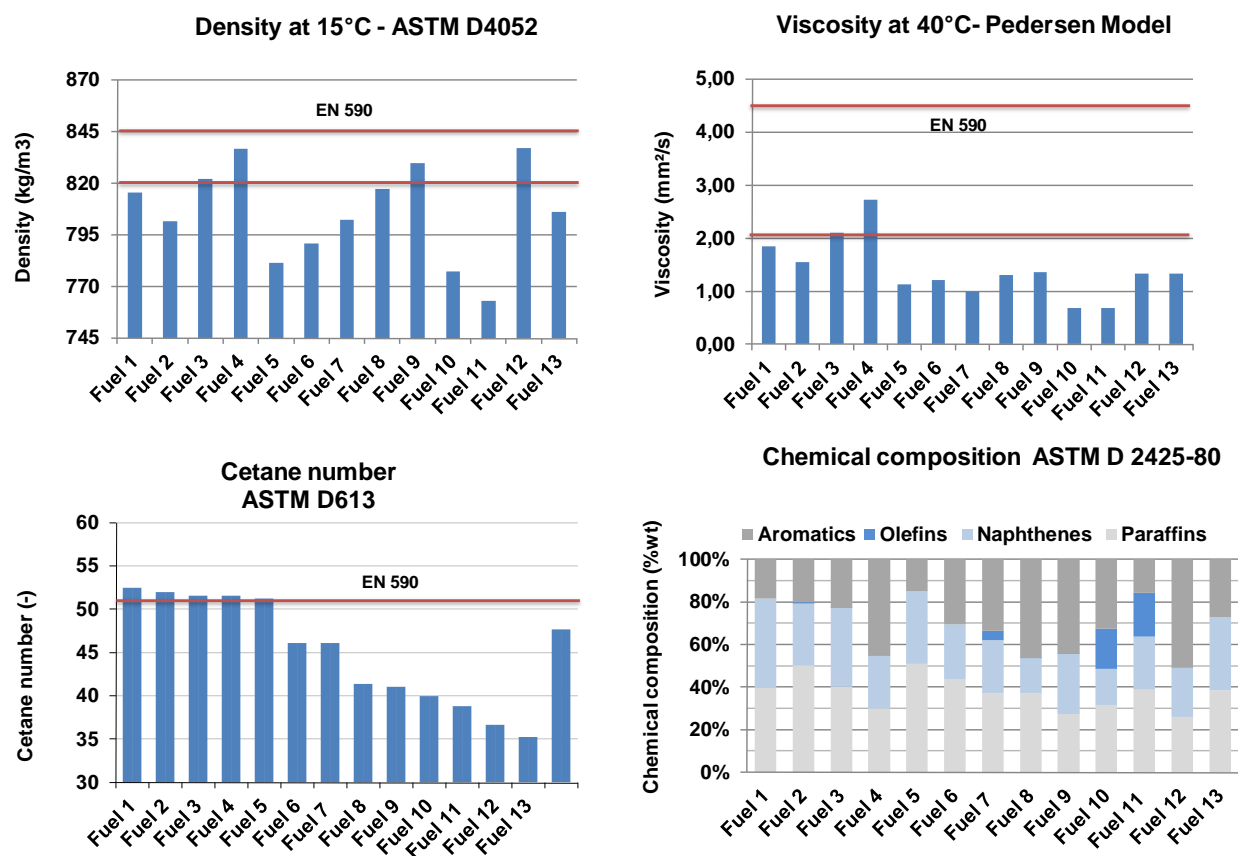
		Unit	Fuel 1	Fuel 2	Fuel 3	Fuel 4	Fuel 5	Fuel 6	Fuel 7	Fuel 8	Fuel 9	Fuel 10	Fuel 11	Fuel 12	Fuel 13
Stream composition	HSRG	%vol	0.0	0.0	0.0	0.0	50.0	50.0	9.7	0.0	0.0	0.0	0.0	0.0	20.0
	HFCC	%vol	0.0	1.7	0.0	0.0	0.0	0.0	11.6	0.0	0.0	46.9	50.0	0.0	0.0
	REF	%vol	0.0	0.0	7.4	0.0	0.0	0.0	11.3	20.0	20.0	0.0	0.0	40.8	0.0
	HSRK	%vol	0.0	50.0	0.0	0.0	0.0	0.0	13.4	50.0	0.0	0.0	0.0	0.0	0.0
	HCKK	%vol	50.0	0.0	0.0	0.0	0.0	0.0	11.9	0.0	50.0	0.0	0.0	0.0	50.0
	HSRD	%vol	0.0	0.0	0.0	100.0	0.0	50.0	19.8	30.0	30.0	53.1	0.0	0.0	30.0
	HCKLD	%vol	50.0	48.3	92.6	0.0	50.0	0.0	22.3	0.0	0.0	0.0	50.0	59.2	0.0
Analyses	Method	Unit													
Density at 15°C	ASTM D4052	kg/m ³	815.6	801.5	822	836.6	781.4	790.7	802.3	817.4	829.8	777.1	763.1	837.2	806
Kin. viscosity 40°C	EN ISO3105	mm ² /s	1.85	1.55	2.11	3.297	1.12	1.21	0.99	1.31	1.36	0.68	0.69	1.33	1.33
Sulfur	EN ISO 20846	mg/kg	1	111	1	2	1	1	31	111	1	3	3	1	1
LHV	ASTM D240	MJ/kg	42.97	43.29	43.13	41.83	41.22	42.79	42.12	42.29	42.65	40.12	40.20	41.95	42.67
CN (CFR)	ASTM D613	-	52.0	51.6	51.6	51.2	46.1	46.1	41.4	41.1	40.0	38.8	36.7	35.2	47.7
H/C/N/O															
C		%wt	86.08	85.90	86.32	86.25	85.68	85.81	86.48	86.89	87.07	86.08	85.94	87.84	86.04
H		%wt	13.76	13.95	13.47	13.75	14.21	14.19	13.44	13.06	12.88	13.91	13.95	12.02	13.91
N		%wt	0.06	0.10	0.11	0.00	0.06	0.00	0.04	0.05	0.00	0.00	0.06	0.07	0.00
O		%wt	0.11	0.05	0.10	0.00	0.06	0.00	0.04	0.00	0.06	0.00	0.06	0.07	0.06
H/C		%wt	1.92	1.95	1.87	1.91	1.99	1.98	1.87	1.80	1.77	1.94	1.95	1.64	1.94
Composition	GCxGC														
Paraffins		%wt	39.9	50.0	40.2	29.9	50.8	43.6	36.9	37.1	27.2	31.3	38.7	26.0	38.5
Naphtenes		%wt	41.6	29.0	37.1	24.6	34.0	25.8	25.0	16.5	28.5	17.2	25.0	23.3	34.4
Olefins		%wt	0.0	0.7	0.0	0.0	0.0	0.0	4.5	0.0	0.0	19.0	20.6	0.1	0.0
Monoaromatics		%wt	17.1	18.9	21.1	41.7	14.3	28.7	32.0	44.5	42.4	30.5	14.8	49.4	25.4
Polyaromatics		%wt	1.5	1.3	1.6	3.6	0.9	1.8	1.5	1.7	1.8	1.9	0.9	1.3	1.7
Total Aromatics		%wt	18.5	20.3	22.7	45.3	15.2	30.5	33.5	46.3	44.2	32.4	15.7	50.7	27.1
Distillation	ASTM D2887														
IBP		°C	161	36	129	202	99	98	36	130	130	36	36	125	98
T50		°C	233	231	267	292	190	197	201	197	205	197	201	212	208
T95		°C	306	326	314	380	306	375	382	369	369	401	328	307	353

169

170 Figure 3 illustrates the density, viscosity, cetane number and PONA composition of the fuels in the matrix.

171 Diesel-rich and reformate-rich fuels (Fuel 3, 4, 8, 9 and 12) have the higher density, while the lowest

172 density ones have higher fraction of HSRG and HFCC gasoline streams. Several matrix fuels are under the
 173 range of the European specification EN590 (820-845 g/L). Due to the high volatility of several fuels,
 174 viscosity could not be measured in the standard 40°C temperature. Pedersen model [31] (validated at 10°C
 175 with a correlation coefficient of 0.93) was used to estimate viscosity at 40°C. Calculated viscosity at 40°C
 176 is significantly low for the entire matrix compared with European specification EN 590, except for diesel-
 177 rich fuels.



178

179 *Figure 3: Density, Viscosity at 40°C (Pedersen model), cetane number and chemical composition of the*
 180 *fuel matrix Fuels 1-12 and the validation fuel (Fuel 13)*

181 PONA composition of the matrix fuels was calculated by linear correlation from the data of single streams
 182 (Appendix A). Paraffinic compounds (linear and branched) vary from 26 to 51%wt. Aromatics range from
 183 15 to 51%wt. Olefins are present in HFCC containing fuels: i.e. Fuels 2, 7, 10 and 11. They range from 2
 184 to 21%wt. Finally, naphthenes range from 16 to 42%wt. Volatility is the highest for Fuels 2, 10 and 11,

185 due to HFCC presence even at very low ratio, and Fuels 3 and 5 most likely due to the presence of
186 HCKLD whose IBP is close to gasoline streams.

187 **2.3 Fuel optimization procedure**

188 The experiments were conducted in a DV6D 4-cylinder light duty diesel engine from PSA Peugeot
189 Citroën (PSA), compliant with Euro 5 specification. The engine details are given in Table 2. The engine
190 oil and water temperatures were set to 90°C during the experiment. The engine was equipped with a
191 Bosch CRI2.2 common rail direct fuel injection with a maximum rail pressure of 1800 bar, a turbocharger
192 with a fixed geometry and a high pressure EGR system. The engine was tested without the after-treatment
193 system fitted and an open Engine Control Unit (ECU) was used to monitor injection parameters and
194 air/EGR settings.

195 *Table 2: Details of the DV6D 4-cylinder engine model from PSA*

Engine specifications	Value
Bore	75 mm
Stroke	88,3 mm
Displacement	1560 cm ³
Connecting rod length	136,8 mm
Compression ratio	16:1
Intake valve opening	377 °CA
Intake valve closing	550 °CA
Intake valve maximum lift	9,25 mm
Exhaust valve opening	164°CA
Exhaust valve closing	350°CA
Exhaust valve maximum lift	9,25 mm
Maximum torque	230 Nm at 1750 rpm
Maximum Power	68 kW at 4000 rpm

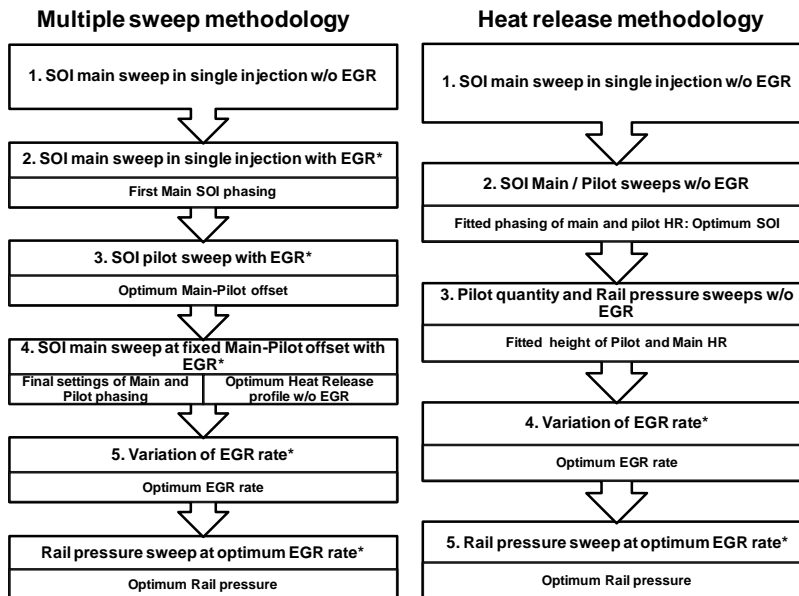
196 The experiment was conducted in double injection mode (i.e. pilot and main injection) with EGR. To cope
197 with the high dispersion of fuels properties, particularly volatility and reactivity, the engine settings were
198 adapted for each fuel. Matrix fuels were optimized separately on six operating points ranging from 1350 to
199 2400 rpm engine speed and from 1 to 13.4 bar of Brake Mean Effective Pressure (BMEP). These
200 operating points are representative of the New European Driving Cycle (NEDC) and have been used to
201 evaluate new formulation or engine concepts for reduced pollutants emissions by other groups [32], [9].
202 To better illustrate the main results, we present in this article two engine operating points selected in the
203 light and middle load; 1500 rpm - 6 bar (EP1) and 2280 rpm – 8.2 bar (EP2). Both engine operating points
204 are optimized using the same methodology for each fuel, allowing the definition successively of the
205 optimum settings of main and pilot injections phasing, pilot quantity, EGR rate and rail pressure. The
206 intake pressure was fixed to PSA’s standard calibration matching the maximum engine capacity. Pilot
207 quantity was fixed to 1.5mg/stroke, corresponding to the average pilot quantity used in the stock
208 calibration. To reduce the optimization time, the fuels were categorized into three cetane ranges (Group 1:
209 47-52, Group 2: 41-46 and Group 3: 35-40). Within each range, a “central” fuel was defined: Fuel 4, Fuel
210 7 and Fuel 11, respectively. Central fuels were optimized with a detailed method consisting of successive
211 single parametric variations of main and pilot injection phasing, rail pressure and EGR rate. The optimum
212 parameters are defined to achieve targets of NO_x, PM, noise, CO, HC and IMEP stability (summarized in
213 Table 3) compliant with levels obtained in Euro 5-6 regulations, using similar test equipment [9]. The
214 final optimized heat release profile was used as a baseline for the optimization of the fuels belonging to
215 the same cetane group. An overview of both methodologies is provided in Figure 4. Note that the injection
216 pressure was optimized for each fuel separately. The initial rail pressure for the “central” fuels (used in the
217 optimization methodology) was that of the standard map, i.e. 800 bar for EP1 and 1146 bar for EP2, while,
218 for the fuels belonging to the same cetane group, the initial rail pressure corresponds to the optimized
219 pressure of the “central” fuel. It should be noted that fixed engine settings such as the intake pressure
220 correspond to diesel like-fuels, and may influence the results of high volatility and low-cetane number
221 fuels. For example, a higher intake may better highlight the potential of high volatility and low-cetane

222 number fuels according to previous work of Han et al. [17]. Further details on the optimization
 223 methodology are provided in Appendix B.

224 *Table 3: Engine optimization criteria at 1500 rpm – 6 bar (EP1) and 2280 rpm – 8.2 bar (EP 2). (*) Fuel*
 225 *consumption is minimized if the pollutant targets are respected*

Parameter	Unit	Precision	Fixed settings and optimization criteria	
			1500 rpm	2280 rpm
Engine speed	rpm	+/- 3	1500	2280
Engine load	bar	+/- 0.1	6	8.2
Intake pressure	bar	+/- 0.015	1.03	1.46
NOx	g/kWh	+/- 0.03	Minimize	Minimize
Particles	g/kWh	+/- 0.03	< 0.15	<0.2
CO	g/kWh	+/-1	< 8	<4
HC	g/kWh	+/-0.1	< 0.8	<0.4
COV	%	+/- 0.5	3	3
Noise	dB	+/- 1	85	89

226



227

228 *Figure 4: Overview of the optimization methodologies (*) optimum levels were determined in agreement*
 229 *with the target and constraints described in Table 3*

230 **2.4 NO_x - PM tradeoff characterization**

231 To characterize the NO_x-PM tradeoff, a quantified evaluation developed. Based on the NO_x and PM
232 emissions measured during the final EGR sweep, exponential curves representing PM emissions as a
233 function of NO_x (Figure 5) were fitted according to the following equation: $PM(g/kWh) =$
234 $A(i,j) \exp(B(i,j)/NO_x(g/kWh))$, where A and B are fitting coefficients determined for the fuel i and
235 operation point j. The correlation coefficients are above 0.95 for all matrix fuels optimized at different
236 speed-load conditions. The integral of the curves (C_{PM}), calculated over a determined NO_x range, allowed
237 the characterization of the NO_x-PM tradeoff. Fuels having a better NO_x-PM tradeoff would have a lower
238 level of PM integral (or cumulated particulates) over the integration domain. The robustness of this
239 evaluation was checked through a variation of the integration limits. This method for NO_x-PM tradeoff
240 characterization aims to complete the more conventional optimum selection and point-to-point
241 comparison. The latter may not be representative of the overall fuel behavior and may not be indicative of
242 a fuel's sensitivity to small variation in engine settings, especially intake O₂ concentration. This method is
243 usually poorly discriminating in the case of small differences.

244 **3 Results**

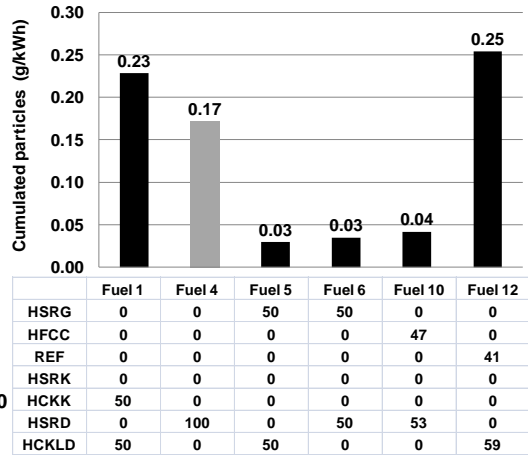
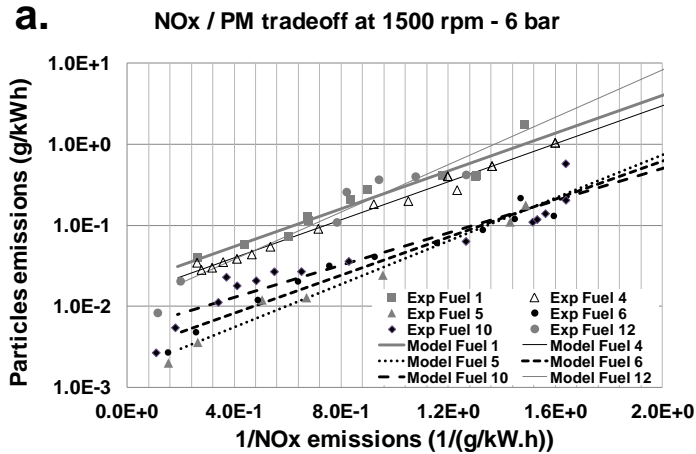
245 **3.1 Fuel matrix evaluation**

246 This section presents the results of the fuel matrix evaluation. To highlight the main fuel effect observed,
247 only matrix fuels composed of binary mixtures with a significant percentage of light gasoline and
248 kerosene streams are presented. Namely, Fuels 2, a diesel/kerosene blend and Fuels 5, 6, 10 and 12, which
249 are gasoline/diesel blends. Fuel 4 composed of 100% HSRD was the reference fuel. Fuels are compared
250 on engine conditions EP1 and EP2. Figure 5 illustrates the comparison of the NO_x-PM tradeoff and
251 cumulated particulates (C_{PM}) over the NO_x optimum range, i.e. from 0.7 to 1.5 g/kW.h and from 1 to 2
252 g/kW.h on EP1 and EP2, respectively (Appendix C). To evaluate the robustness of this approach, the
253 limits of the NO_x range were varied by +/- 0.5 g/kW.h, and results show negligible variation of the main

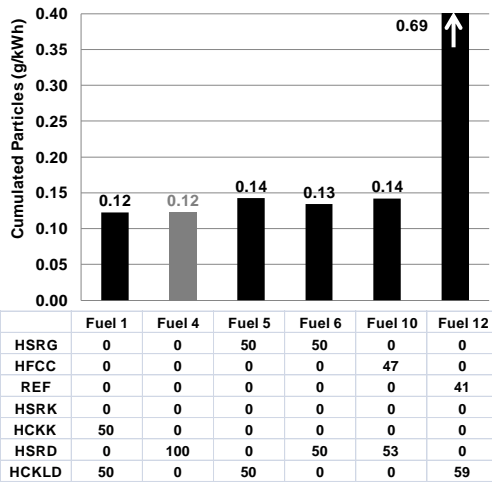
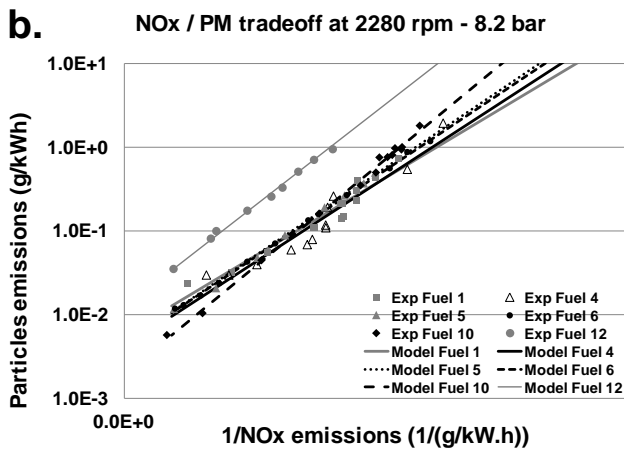
254 trends discussed hereafter. Moreover, optimum results summarized in Figure 6 are discussed to illustrate
255 the variation of fuel consumption and other regulated pollutants with respect to streams composition.
256 Engine results synthesis using the entire fuel matrix is summarized in Appendix C.

257 ***Effect of the addition of Hydrotreated Straight Run Gasoline (HSRG) to Diesel***

258 On EP1, the addition of 50% HSRG to both diesel streams (HSRD or HCKLD, in Fuel 6 and Fuel 5,
259 respectively) allows over 5 times lower C_{PM} compared with reference diesel Fuel 4. Through the
260 combination of fuel's higher volatility and increased ignition delay, HSRG addition shifts the combustion
261 towards the lower temperature range, thus reducing the NO_x emissions. The decrease of PM emissions
262 may be associated with the fuel composition through lower fractions of aromatics and soot precursors
263 especially in Fuel 5, in agreement with the results of Weall et al. investigating gasoline-diesel blends [30].
264 Similar conclusions were obtained by Han et al. [17], [16] showing that the addition of gasoline up to
265 40%vol allowed the simultaneous reduction of NO_x and soot emissions. Optimum results comparison
266 (Figure 6) shows a reduction in fuel consumption and HC emissions (5% and 25%, respectively).
267 However, carbon monoxide increased by 30% and 85%, for Fuel 5 and Fuel 6, respectively compared with
268 Fuel 4. Lower fuel consumption can be associated with the shorter combustion duration (CA₉₀-CA₁₀ is
269 half of that of diesel fuel), while the CO increase is mainly due to lower combustion efficiency typical of
270 low cetane number fuels especially at high EGR rates [33], usually due to over-mixing leading to fuel-lean
271 regions acting as carbon monoxide sources [14]. At the higher engine load of EP2, Fuels 5 and 6 present
272 similar trends and NO_x-PM tradeoff is comparable to Fuel 4.



273

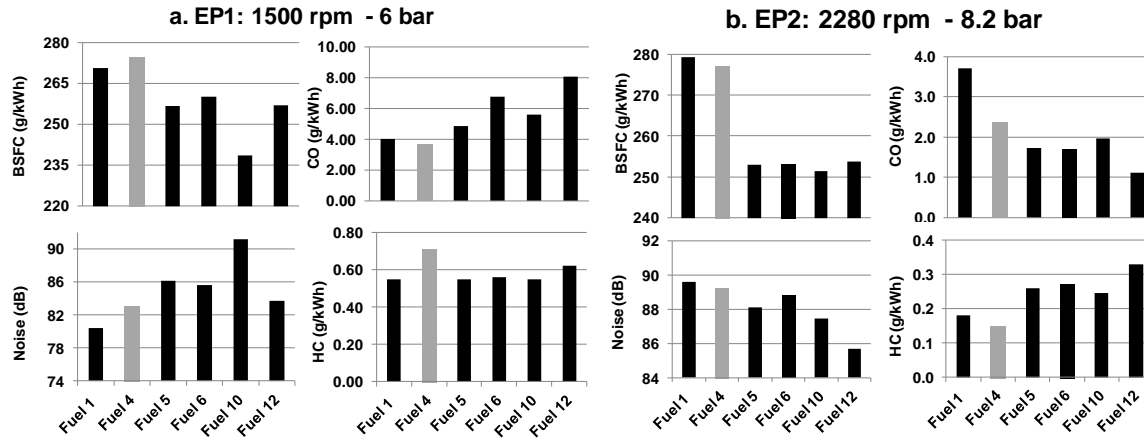


274

275 *Figure 5: NOx-PM tradeoff during EGR sweeps (experiment and model) for several matrix fuels, CPM*
 276 *calculation a) EP1: 1500 rpm-6bar. b) EP2: 2280rpm-8.2 bar*

277

278 This result is closely related to fuel characteristics. Later SOI, applied for diesel fuel allows for shifting
 279 the combustion towards the lower temperature range, whereas, the EGR rate is limited by the soot
 280 constraint. In the case of gasoline/diesel blends (Fuels 5 and 6), SOI is limited by stability, NOx emissions
 281 are lowered through the higher EGR rate possible by virtue of their low sooting tendency. Both strategies
 282 lead to a similar NOx-PM tradeoff, however, Fuels 5 and 6 present the advantage of reduced fuel
 283 consumption, through better combustion phasing and shorter combustion duration favored by better air
 284 fuel mixing.



285

286 *Figure 6: Optimized engine outputs of several matrix fuels tested at two engine conditions: a) EP 1: 1500*
 287 *rpm-6bar and b) EP2: 2280rpm-8.2 bar*

288

289 ***Effect of the addition of Hydrotreated Fluid Catalytic Cracking (HFCC) to Diesel***

290 HFCC addition to HSRD studied in Fuel 10 reduces by over 4 times C_{PM} compared with HSRD. Low CN
 291 contributes to increase the autoignition delay, shifting the combustion towards lower temperatures which
 292 reduces NOx emissions. Additionally, the high volatility reduces the formation fuel rich areas and high
 293 olefin content ensures a high reaction rate [34] thus reducing PM emissions. Both effects allow for
 294 achieving very good NOx-PM tradeoff at EP1. Optimum results at EP1 (Figure 6), illustrate 13% lower
 295 fuel consumption and 23% lower HC emissions compared with Fuel 4. In fact, the higher rate of
 296 combustion of the olefin-rich HFCC stream reduces the combustion duration and favors thermal
 297 efficiency. CO emissions increase by over 45% comparably with the HSRG effect (Fuel 6). We note that
 298 noise level was very high (91 dB) and could not be reduced with the settings variation, most likely due to
 299 the increased autoignition delay and mixture-controlled combustion. At higher load at EP2, Fuel 10
 300 presents roughly similar results to Fuel 4 in terms of NOx-PM tradeoff, CO, HC and noise. However, a
 301 better fuel economy is achieved mainly due to better phasing and shorter combustion promoted by better
 302 mixing.

303

304 ***Effect of the addition of Reformate (REF) to Diesel***

305 The addition of around 40% REF to HCKLD in Fuel 12 leads to a significant degradation in the C_{PM}
306 performance (8 times higher than the HSRG/HCKLD mixture and 50% higher than reference diesel). This
307 trend can be attributed to the low CN of Fuel 12 and the low combustion stability that limits EGR
308 capacity. Both contribute to NO_x formation through increased mixture-controlled high temperature
309 combustion, thus, confirming a negative effect of excessive ignition delay on exhaust emissions observed
310 by other groups [35]. Moreover, the higher aromatic fraction provided by the REF stream contributes to an
311 increase in the soot precursors and can also play a role in increasing NO_x formation [24]. Contrary to the
312 HSRG and HFCC effect on NO_x-PM, which drops off at higher load, the negative effect of REF addition
313 to diesel is more pronounced at higher load (Figure 5). A fair linear relationship between C_{PM} and REF
314 volume fraction is obtained. Optimum results show a similar positive trend on fuel consumption on EP1
315 and EP2 and CO emissions increase on EP1 in agreement with the other gasoline streams.

316 ***Effect of the addition of Hydrocracked Kerosene (HCKK) to Diesel***

317 The addition of HCKK kerosene stream to HCKLD in Fuel 1 leads to an increase in C_{PM} by over 7 times
318 compared with HSRG in the same proportion (Fuel 5) at EP1. Its lower volatility and higher cetane
319 number reduces the mixing efficiency and favors the formation of fuel-rich areas which increases the
320 sooting tendency. The fuel chemistry can also contribute to a NO_x rise through lower paraffin and higher
321 naphthenes fractions. The NO_x relationship to the molecular structure of alkanes studied in literature
322 shows higher NO_x tendency for cyclic paraffins compared to normal and branched ones [24][36]. At
323 higher load, the addition of HCKK has a relatively small impact on NO_x-PM tradeoff. Optimum results
324 presented in Figure 6 illustrate higher fuel consumption at EP1 and EP2, and reduced CO emissions at
325 EP1 which confirms the previous hypothesis. Overall, we observe that kerosene/diesel blends behave
326 similarly to diesel streams in terms of engine efficiency and regulated pollutants.

327

328 **Summary**

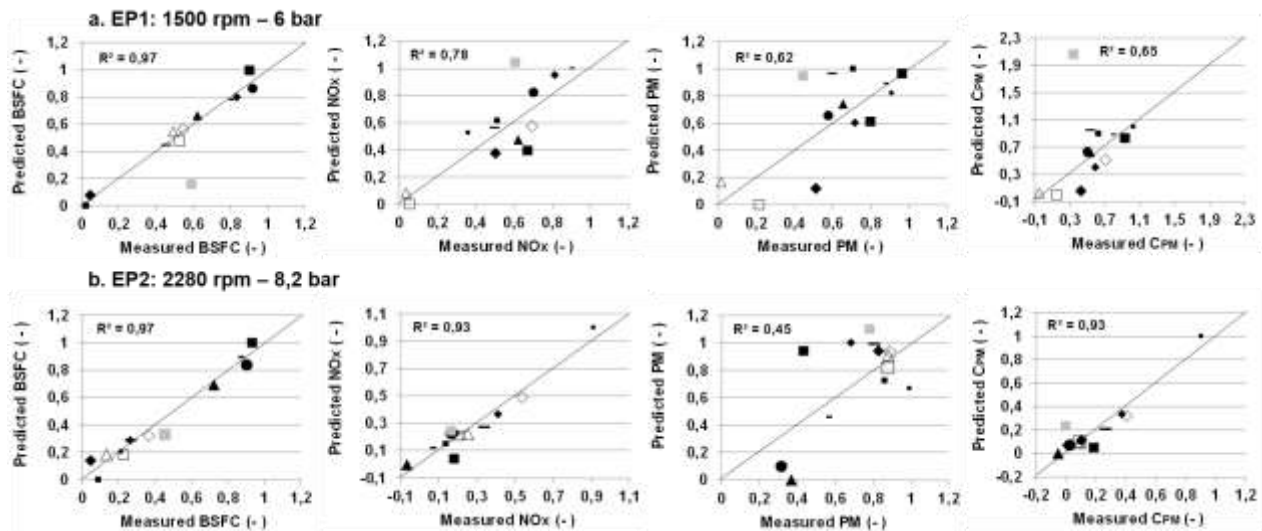
329 The analysis of engine results allows a first evaluation of both the direct and synergistic effects of refinery
330 streams on engine outputs. The results suggest a significant impact of gasoline streams composition on the
331 NO_x/PM/fuel economy trade off. REF addition to diesel streams appears to degrade the NO_x-PM tradeoff
332 at both engine loads. HSRG illustrates a good potential for simultaneously reducing NO_x, PM and fuel
333 consumption with an acceptable increase of carbon monoxide at light load. The addition of olefins-rich
334 HFCC to HSRD diesel streams is also favorable for NO_x / PM trade-off at light load. Finally, the HCKK
335 stream shows diesel-like behavior at light and high load, with rather degraded CO emissions. Results show
336 a sensitivity of the NO_x-PM tradeoff to streams composition which varies with the engine load: lower
337 load engine conditions, characterized by higher homogeneity, are more sensitive to the fuel properties than
338 higher load conditions.

339 **3.2 Modeling of engine outputs and optimization function of the refinery**
340 **streams composition**

341 Linear models with no interaction were built linking optimum results obtained at EP1 and EP2 to the
342 refinery streams' volume fractions. Figure 7 presents predicted and experimental results for several engine
343 outputs of matrix fuels (Fuels 1-12) along with the validation fuel (Fuel 13). Results are normalized from
344 0 to 1 at the scale of all the experimental results. Details of the model coefficients and statistical data are
345 summarized in Appendix D.

346 Fuel consumption has a determination coefficient (R^2) above 0.97 for both EP 1 and EP2; Results of Fuel
347 13 overestimate fuel consumption by 8% for EP1 and are fairly predictive for EP2. NO_x and PM models
348 have low determination coefficients (0.78 and 0.62 respectively for EP1 and 0.93 and 0.45, respectively
349 for EP2). The poor performance of the PM model at EP2 can be associated with the quasi-equity of
350 particulate emissions at the optimum point for most fuels (Appendix C). The models accurately predict
351 EP2 NO_x level for Fuel 13 and within twice the standard deviation interval (σ) for EP1. PM emissions are

352 within twice (σ) at both operating points. The quality of the CO and HC emissions models was good for
 353 EP2 and fair for EP1 (Appendix D). Fuel 13 results were fairly predicted for both. Finally, the model of
 354 $C_{PM_2.5}$ was fair on EP1 ($R^2=0.65$) and good on EP2 ($R^2=0.93$). The prediction of Fuel 13 level was fair only
 355 for EP2 and poor for EP1.

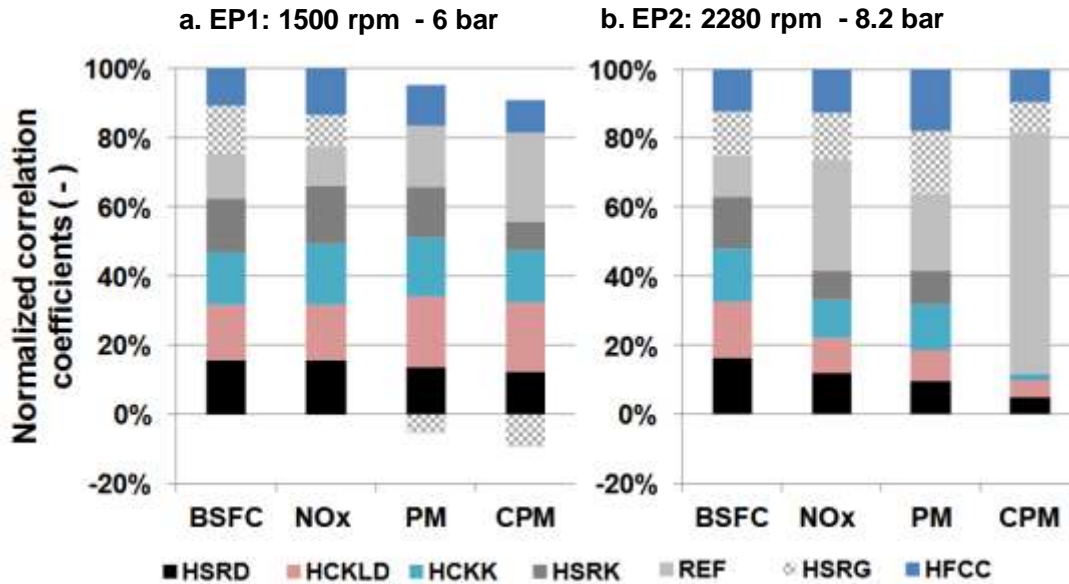


356
 357 *Figure 7: Modeling of the engine outputs based on optimum results at EP1 (1500rpm – 6 bar) and EP2*
 358 *(2280 rpm-8.2 bar). Symbols: (-): Fuel 1, (◆): Fuel 2, (■): Fuel 3, (●): Fuel 4, (□): Fuel 5, (Δ): Fuel 6,*
 359 *(—): Fuel 7, (▲) Fuel 8, (◇): Fuel 9, (◆): Fuel 10, (■): Fuel 11, (●): Fuel 12 and (Gray ■) Fuel 13.*

360
 361 Figure 8 presents the normalized correlation coefficients. They illustrate the contribution of the different
 362 refinery streams to fuel consumption, NOx and particulates on EP1 and EP2. **Fuel consumption**
 363 **coefficients** are similar for EP1 and EP2 where diesel and kerosene streams have higher coefficients
 364 compared with gasoline streams and in agreement with the previous analysis. At light load, HSRG and
 365 HFCC streams reduces heat rejection through lower combustion temperature, while at mid load, they
 366 induce later and higher temperature premixed combustion, thus increasing the combustion efficiency
 367 (Figure 6). **NOx coefficients** vary significantly between EP1 and EP2. EP 1 presents a higher sensitivity to

368 streams composition. The lowest coefficients are associated with HSRG and REF, then HFCC, while
369 diesel and kerosene streams are more similar, confirming previous conclusions. At higher load, HFCC and
370 HSRG streams' coefficients become higher than both kerosene and diesel, although of a similar
371 magnitude. REF has the worst effect on NOx emissions, three times higher than standard diesel and over
372 twice as high as the other gasoline streams. *PM coefficients* are lower for gasoline streams HSRG and
373 HFCC at light load and tend to increase at mid load. Only REF presented high PM coefficients for both
374 EP1 and EP2. HSRD and kerosene streams present a good tradeoff with average levels at EP1 and EP2.
375 The *coefficients of the C_{PM}* model, in agreement with the previous analysis of NOx and PM coefficients,
376 underline the negative effect of REF stream on EP1 and more significantly on EP2, and the suitability of
377 gasoline streams HSRG and HFCC at light load with low coefficients and kerosene and diesel streams at
378 mid load.

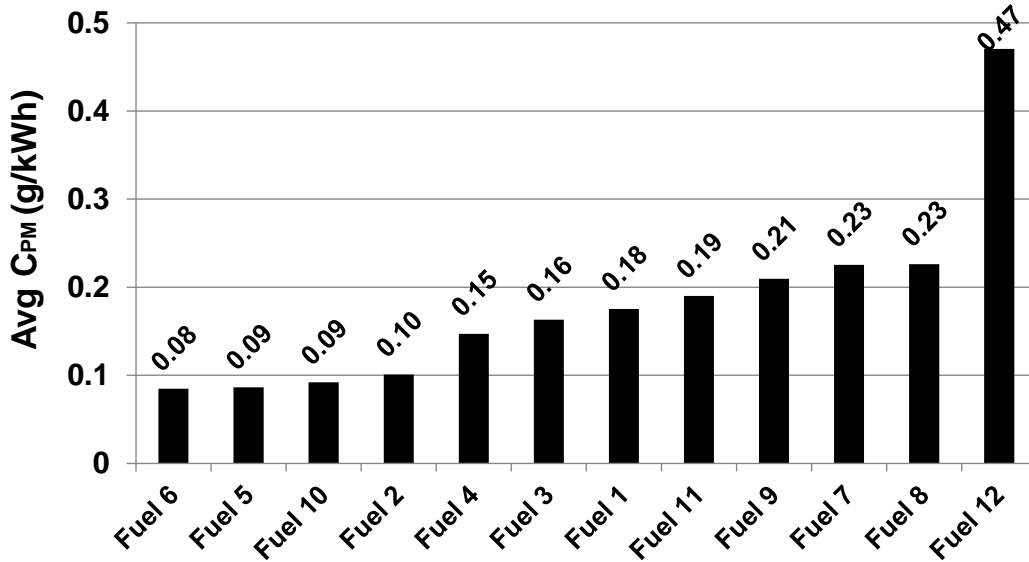
379 To summarize, modeling of the engine outputs allows qualitative representation of the main streams
380 effects described in section 2.1. The models' accuracy was fair for several engine outputs over the tested
381 conditions, however not sufficiently predictive for the results of the validation fuel. This may be
382 associated to the relatively low number of fuels used to build the model. Besides, the model did not take
383 into account streams' interactions, that may have an influence as well. Therefore, two approaches were
384 evaluated, for fuel optimization, first, through the minimization of pollutants (NOx and PM trade off),
385 then through a comparative evaluation of the optimized fuel with matrix fuels.



386

387 *Figure 8: Normalized correlation coefficient of the linear model for a. EP 1 and b. EP 2 function of the*
 388 *volume fraction of the refinery streams*

389 Based on the developed models, an optimization was carried out, aimed at proposing a streams
 390 composition allowing for the best NO_x-PM tradeoff through the minimization of C_{PM} criterion averaged
 391 on EP1 and EP2 $C_{PM} = \frac{C_{PM}(EP1) + C_{PM}(EP2)}{2}$. The optimization was carried out under the same constraints
 392 on EP1 and EP2 for PM, CO, HC and stability adopted for the matrix fuel evaluation methodology (Table
 393 3). Interestingly, the optimum composition is one of the matrix fuels tested: Fuel 6, a diesel/gasoline blend
 394 composed of 50%v HSRD and 50%v HSRG, in good agreement with the ranking of the fuels according to
 395 average C_{PM} displayed in Figure 9. This fuel allows, at light load, a drastic reduction in NO_x emissions
 396 and a low sooting tendency, and a fairly good behavior at mid load.



397
 398 *Figure 9: Ranking of the fuel matrix according to NO_x-PM Tradeoff: Average of C_{PM} on EP1 and EP2*

399 **4 Conclusions**

400 In this study, we propose an original methodology to optimize the fuel formulation for compression
 401 ignition light-duty engines, to achieve lower pollutants emissions and higher engine efficiency based on a
 402 DoE approach. Seven refinery streams representative of gasoline, kerosene and diesel cuts are used. A D-
 403 Optimal mixture design was applied to build, a 12-run, 7-factor fuel matrix. Fuels were thoroughly
 404 optimized on light and mid load engine points representative of typical vehicle running conditions. The
 405 results show a high sensitivity of the engine efficiency and pollutants emissions to streams composition.
 406 Optimal fuel requirements varied as a function of the engine operating point. At light load, the addition of
 407 up to 50% gasoline streams (mainly HSRG) to diesel streams demonstrates a better potential to achieve
 408 simultaneously low NO_x and PM emissions and an overall good engine performance. Reformate, a highly
 409 aromatic gasoline stream, did not offer an advantage at any of the tested conditions due to high particulate
 410 emissions. The two kerosene streams evaluated in this work performed similarly to diesel streams in terms
 411 of engine efficiency and pollutants emissions. A compromise fuel is proposed composed of 50%vHSRG

412 and 50%vHSRD that allows halving of NO_x and PM emissions and reducing of fuel consumption by
413 5%wt compared to reference diesel HSRD.

414 This study allowed to put forward an interesting potential of using gasoline and kerosene streams in diesel
415 fuels on a commercial light-duty diesel engine (PSA DV6D). The optimization methodology was based on
416 reduced number of parameters and interactions. A more elaborated engine calibration would be necessary
417 to confirm the observed trends on larger range of operating conditions. Besides, the upgrading of the
418 engine hardware (especially, in terms of boost pressure and combustion chamber design) may allow to
419 further explore the full potential of these streams in terms of engine performance and emissions.

420 **5 Acknowledgement**

421 Authors acknowledge the valuable support of Saudi Aramco to this research work and would like to thank
422 Romain CHERBLAND and Yoan LEMONNIER from IFP Energies Nouvelles for conducting the engine
423 experiments and Frederic NICOLAS from IFP Energies Nouvelles for engine calibration support.

424 **6 References**

- 425 [1] “EU Transport in Figures - Statistical Pocketbook 2014,” European Commission, Tech. Rep.,
426 2014.
- 427 [2] A. Capros, N. Devitan, and T. D. et al, “EU Energy, Transport and GHG emissions Trends to
428 2050, Reference scenario 2013,” European commission, Tech. Rep., 2013.
- 429 [3] R. H. Stanglmaier and C. E. Roberts, “Homogeneous charge compression ignition (HCCI):
430 benefits, compromises, and future engine applications,” SAE Technical Paper, Tech. Rep., 1999.
- 431 [4] M. Christensen, A. Hultqvist, and B. Johansson, “Demonstrating the Multi Fuel Capability of a
432 Homogeneous Charge Compression Ignition Engine with Variable Compression Ratio,” *SAE Technical*
433 *Paper*, vol. 1999-01-3679, 1999.
- 434 [5] L. Pesant and L. Forti, “IFP International consortium Effects of fuel and additives on diesel HCCI
435 engines, 4th year, final report,” IFPEN, Tech. Rep., 2008.
- 436 [6] M. Muether, M. Lamping, A. Kolbeck, R. F. Cracknell, D. J. Rickeard, and K. D. Rose,
437 “Advanced Combustion for Low Emissions and High Efficiency Part 1: Impact of Engine Hardware on
438 HCCI Combustion,” *SAE Technical Paper*, vol. 2008-01-2405, 2008.
- 439 [7] C. Noehre, M. Andersson, B. Johansson, and A. Hultqvist, “Characterization of partially premixed
440 combustion,” SAE Technical Paper, Tech. Rep., 2006.
- 441 [8] G. T. Kalghatgi, P. Risberg, and H.-E. Angstrom, “Partially Pre-Mixed Auto-Ignition of Gasoline
442 to Attain Low Smoke and Low NOx at High Load in a Compression Ignition Engine and Comparison with
443 a Diesel Fuel,” *SAE Technical Paper*, vol. 2007-01-0006, 2007.

- 444 [9] A. Warey, J.-P. Hardy, M. Hennequin, M. Tatur, D. Tomazic, and W. Cannella, "Fuel Effects on
445 Low Temperature Combustion in a Light-Duty Diesel Engine," *SAE Technical Paper*, vol. 2010-01-1122,
446 2010.
- 447 [10] T. Zannis and D. Hountalas, "Effect of fuel aromatic content and structure on direct-injection
448 diesel engine pollutant emissions," *Journal of the Energy Institute*, vol. 77, no. 511, pp. 16–25, 2004.
- 449 [11] R. F. Cracknell, D. J. Rickeard, J. Ariztegui, K. D. Rose, M. Muether, M. Lamping, and
450 A. Kolbeck, "Advanced Combustion for Low Emissions and High Efficiency Part 2: Impact of Fuel
451 Properties on HCCI Combustion," *SAE Technical Paper*, vol. 2008-01-2404, 2008.
- 452 [12] A. S. E. Cheng, B. T. Fisher, G. C. Martin, and C. J. Mueller, "Effects of Fuel Volatility on Early
453 Direct-Injection, Low-Temperature Combustion in an Optical Diesel Engine," *Energy & Fuels*, vol. 24,
454 no. 3, pp. 1538–1551, 2010. [Online]. Available: <http://pubs.acs.org/doi/abs/10.1021/ef9011142>
- 455 [13] P. Miles, "Sources and mitigation of CO and UHC emissions in low-temperature diesel
456 combustion regimes: Insights obtained via homogeneous reactor modeling," in *13th Diesel Engine
457 Efficiency and Emissions Research Conference, August 13-16, Detroit, Michigan, 2007*.
- 458 [14] M. P. Musculus, T. Lachaux, L. M. Pickett, and C. A. Idicheria, "End-of-injection over-mixing
459 and unburned hydrocarbon emissions in low-temperature-combustion diesel engines," *SAE Technical
460 Paper, Tech. Rep.*, 2007.
- 461 [15] S. M. Aceves, D. L. Flowers, C. K. Westbrook, J. R. Smith, W. Pitz, R. Dibble, M. Christensen,
462 and B. Johansson, "A multi-zone model for prediction of HCCI combustion and emissions," *SAE
463 Technical paper, Tech. Rep.*, 2000.
- 464 [16] D. Han, A. M. Ickes, S. V. Bohac, Z. Huang, and D. N. Assanis, "Premixed low-temperature
465 combustion of blends of diesel and gasoline in a high speed compression ignition engine," *Proceedings of*

466 *the Combustion Institute*, vol. 33, no. 2, pp. 3039 – 3046, 2011. [Online]. Available: [http://-](http://www.sciencedirect.com/science/article/pii/S1540748910003081)
467 www.sciencedirect.com/science/article/pii/S1540748910003081

468 [17] D. Han, A. M. Ickes, D. N. Assanis, Z. Huang, and S. V. Bohac, “Attainment and Load Extension
469 of High-Efficiency Premixed Low-Temperature Combustion with Dieseline in a Compression Ignition
470 Engine,” *Energy & Fuels*, vol. 24, no. 6, pp. 3517–3525, 2010. [Online]. Available: [http://pubs.acs.org/-](http://pubs.acs.org/doi/abs/10.1021/ef100269c)
471 [doi/abs/10.1021/ef100269c](http://pubs.acs.org/doi/abs/10.1021/ef100269c)

472 [18] P. Risberg, G. Kalghatgi, H.-E. Ångström, and F. Wåhlin, “Auto-ignition quality of diesel-like
473 fuels in HCCI engines,” SAE Technical Paper, Tech. Rep., 2005.

474 [19] P. Bergstrand, “Effects on combustion by using kerosene or MK1 diesel,” SAE Technical Paper,
475 Tech. Rep., 2007.

476 [20] A. P. Singh and A. K. Agarwal, “Dieseline, Diesohol and Diesosene Fuelled HCCI Engine
477 Development,” SAE Technical Paper, Tech. Rep., 2015.

478 [21] K. Nakakita, H. Ban, S. Takasu, Y. Hotta, K. Inagaki, W. Weissman, and J. T. Farrell, “Effect of
479 hydrocarbon molecular structure in diesel fuel on in-cylinder soot formation and exhaust emissions,” SAE
480 Technical Paper, Tech. Rep., 2003.

481 [22] J. Song and K. O. Lee, “Fuel Property Impacts on diesel particulate morphology, nanostructures,
482 and NO_x emissions,” SAE Technical Paper, Tech. Rep., 2007.

483 [23] Y. Takatori, Y. Mandokoro, K. Akihama, K. Nakakita, Y. Tsukasaki, S. Iguchi, L. I. Yeh, and
484 A. M. Dean, “Effect of Hydrocarbon Molecular Structure on Diesel Exhaust Emissions Part 2: Effect of
485 Branched and Ring Structures of Paraffins on Benzene and Soot Formation,” in *SAE Technical Paper*.
486 SAE International, 10 1998. [Online]. Available: <http://dx.doi.org/10.4271/982495>

- 487 [24] F. Bachmaier, K. Eberius, and T. Just, "The formation of nitric oxide and the detection of HCN in
488 premixed hydrocarbon-air flames at 1 atmosphere," *Combustion Science and Technology*, vol. 7, no. 2, pp.
489 77–84, 1973.
- 490 [25] S.-S. Kee, A. Mohammadi, Y. Kidoguchi, and K. Miwa, "Effects of Aromatic Hydrocarbons on
491 Fuel Decomposition and Oxidation Processes in Diesel Combustion," in *SAE Technical Paper*. SAE
492 International, 05 2005. [Online]. Available: <http://dx.doi.org/10.4271/2005-01-2086>
- 493 [26] M. Al-Abdullah, G. Kalghatgi, and H. Babiker, "Flash points and volatility characteristics of
494 gasoline/diesel blends," *Fuel*, vol. 153, pp. 67 – 69, 2015. [Online]. Available: [http://-](http://www.sciencedirect.com/science/article/pii/S0016236115002239)
495 www.sciencedirect.com/science/article/pii/S0016236115002239
- 496 [27] M. Castagne, Y. Bentolila, F. Chaudoye, H. A., F. Nicolas, and D. Sinoquet, "Comparison of
497 different calibration methods based on design of experiments," *Oil & Gas Science and Technology - Rev.*
498 *IFP*, vol. 63, no. 4, pp. 563–582, 2008. [Online]. Available: <http://dx.doi.org/10.2516/ogst:2008029>
- 499 [28] R. T. Butts, D. Foster, R. Krieger, M. Andrie, and Y. Ra, "Investigation of the Effects of Cetane
500 Number, Volatility, and Total Aromatic Content on Highly- Dilute Low Temperature Diesel
501 Combustion," *SAE Technical Paper*, vol. 2010-01-0337, 2010.
- 502 [29] M. J. Anderson, *Design-Expert Software V9 Tutorials*. Stat-Ease, Inc., 2014.
- 503 [30] A. Weall and N. Collings, "Investigation into Partially Premixed Combustion in a Light-Duty
504 Multi-Cylinder Diesel Engine Fuelled with a Mixture of Gasoline and Diesel," *SAE Technical Paper*, vol.
505 2007-01-4058, 2007.
- 506 [31] K. S. Pedersen, A. Fredenslund, P. L. Christensen, and P. Thomassen, "Viscosity of crude oils,"
507 *Chemical Engineering Science*, vol. 39, no. 6, pp. 1011 – 1016, 1984. [Online]. Available: [http://-](http://www.sciencedirect.com/science/article/pii/0009250984870098)
508 www.sciencedirect.com/science/article/pii/0009250984870098

- 509 [32] J. Chang, G. Kalghatgi, A. Amer, P. Adomeit, H. Rohs, and B. Heuser, "Vehicle Demonstration
510 of Naphtha Fuel Achieving Both High Efficiency and Drivability with EURO6 Engine-Out NO_x
511 Emission," *SAE International Journal of Engines*, vol. 6, no. 1, pp. 101–119, 2013.
- 512 [33] Y. Jeihouni, S. Pischinger, L. Ruhkamp, and T. Koerfer, "Relationship between fuel properties
513 and sensitivity analysis of non-aromatic and aromatic fuels used in a single cylinder heavy duty diesel
514 engine," SAE Technical Paper, Tech. Rep., 2011.
- 515 [34] L. Starck, B. Lecointe, L. Forti, and N. Jeuland, "Impact of fuel characteristics on {HCCI}
516 combustion: Performances and emissions," *Fuel*, vol. 89, no. 10, pp. 3069 – 3077, 2010. [Online].
517 Available: <http://www.sciencedirect.com/science/article/pii/S001623611000253X>
- 518 [35] K. Kitano, R. Nishiumi, Y. Tsukasaki, T. Tanaka, and M. Morinaga, "Effects of Fuel Properties
519 on Premixed Charge Compression Ignition Combustion in a Direct Injection Diesel Engine," *SAE*
520 *Technical Papers*, vol. 2003-01-1815, 05 2003. [Online]. Available: <http://dx.doi.org/10.4271/2003-01-1815>
521 1815
- 522 [36] L. J.C.Y. and M. P.C., "NO_x as a function of fuel for C₁-to-C₁₆ hydrocarbons and methanol
523 burned in a high intensity, lean-premixed, combustion reactor." in *WSS Meeting, Combustion Institute*,
524 1998.
- 525 [37] R. Lugo, V. Ebrahimian, C. Lefebvre, and C. e. a. Habchi, "A Compositional Representative Fuel
526 Model for Biofuels - Application to Diesel Engine Modelling," *SAE Technical Paper*, vol. 2010-01-2183,
527 2010.

528 **7 Appendices**529 *Appendix A: Main properties of the studied refinery streams*

Analyses	Method	Unit	REF	HFCC	HSRG	HCKK	HSRK	HCKLD	HSRD
Density at 15°C	ASTM D4052	kg/m ³	868.4	691.9	741.1	812.2	787.7	818.7	836.6
Viscosity 40°C	EN ISO 3104	mm ² /s	0.5958	0.36	0.5685	1.342	1.122	2.634	3.297
LHV	ASTM D240	MJ/kg	41.03	44.46	44.29	43.89	40.73	43.57	42.57
Sulfur	NF EN ISO 20846	mg/kg	<0.5	5.7	<0.5	<0.5	221	<0.5	1.5
CN (CFR)	ASTM D613	-	6.1*	16.5*	34.8	45.4	49.0	54.9	51.3
H/C/N (IFPEN)	CG								
C		% wt	90.5	85.9	85.4	86.0	85.8	85.8	86.4
H		% wt	9.5	14.1	14.6	13.8	14.1	14.0	13.6
N		% wt					0.09	0.12	
O		% wt				0.11		0.11	
Total		% wt	100.0	100.0	100.0	100.0	100.0	100.0	100.0
H/C		-	1.255	1.970	2.056	1.930	1.971	1.958	1.889
Composition	GCxGC		8535	8533	8534	8532	8531	8536	8537
Paraffins		% wt	2.15	33.1	59.0	36.3	57.2	43.4	29.9
Naphthenes		% wt	0.14	7.0	27	43	18.5	40.2	25
Olefins		% wt	0.17	45.0	0	0	0	0	0
Aromatics		% wt	97.5	14.8	13.9	20.7	24.3	16.4	45.3
Monoaromatics		% wt	96.7	14.8	13.9	19.5	23.3	14.7	41.7
Polyaromatics		% wt	0.8	0.0	0.0	1.2	1	1.7	3.6
Distillation	EN ISO 3405								
0		°C	105.8	30.4	81	166.9	149.9	123.9	187.9
5		°C	119.5	36.9	98	184.6	165.8	207.4	201.3
10		°C	121.5	39	102.1	190.4	169.7	229.8	206.7
15			122.9	40.3	104.9	193.4	173	241.1	213.4
20		°C	124.1	41.4	107.6	196.2	175.6	247.6	220.8
30		°C	126.2	43.7	112.4	200.7	181.1	257.7	240.6
40		°C	128.7	46.3	117	204.3	186.2	264.9	268.5
50		°C	131.6	49.6	122.9	207.5	191.5	271.7	296.7
60		°C	135.1	54.1	129.1	210.9	197.5	278.5	320.1
70		°C	140.2	61.1	135	214.5	205.4	284.7	344.7
80		°C	146.8	72.8	143	219.4	215.9	292.5	362.7
90		°C	156.7	88.9	152.7	226.4	231.6	304	373.6
95		°C	166.9	98.8	160.1	232	244.8	312.4	378.8
100		°C	198.7	115.4	171.2	243.4	267.8	320.2	381
Recovery at 250°C		% v/v				>98	96.3	22.6	33.9

Recovery at 350°C		% v/v				>98	>98	>98	72.3
Residue		% v/v	1.2	0.7	0.9				

530 * The Cetane Number (CN) of the streams is measured using a CFR engine, with 2 or 3
531 repeatability tests except for REF and HFCC that presented a very low reactivity. Their cetane
532 number was evaluated through blending methods with higher CN streams (namely, HSRK,
533 HSRD, HCKLD and HCKK).

534 Viscosity is measured using the standard test method (EN ISO 3104) at 40°C except HFCC (due
535 to high volatility; IBP=30°C). The viscosity of HFCC is calculated using thermodynamic
536 Pedersen model [37].

537 **Appendix B: Engine optimization methodology and targets**

538 In this section, the detailed and simplified method for fuels optimization are evaluated on the same Fuel in
539 order to quantify the sensitivity to the fuels classification into cetane groups of the engine results. Fuel 5
540 having a central cetane number of 46.1 is tested using multiple sweeps method, and Iso-heat release
541 method in Group 1 and Group 2 (i.e. through the imitation of optimum heat release of Fuel 4 and Fuel 7,
542 respectively) at 3 different engine conditions. The comparison of optimum results shows almost 10%
543 variation of BSFC on average. The amplitude of NOx and PM variation according to the optimization
544 methodology is on average 0.14 and 0.03 g/kW.h, respectively. Optimization methodology impacts mostly
545 the noise level due to its tight relationship with the injection settings. As an initial evaluation of the
546 approach, the sensitivity of engine results to the methodology is taken into account as if it were an engine
547 measurement dispersion error.

EP 1 : 1500 rpm - 6 bar									
Fuel reference	BSFC (g/kWh)	NOx (g/kWh)	PM (g/kWh)	CO (g/kWh)	HC (g/kWh)	CO2 (g/kWh)	noise dB	stab %	C PM g/kWh
Fuel 1	271	1.48	0.12	4.00	0.55	848	80	0.85	0.228
Fuel 2	271	1.46	0.09	3.80	0.49	849	83	0.78	0.121
Fuel 3	281	1.22	0.12	7.10	0.59	878	82	0.96	0.217
Fuel 4	274	1.40	0.09	3.65	0.71	860	83	1.90	0.171
Fuel 5	257	1.05	0.02	4.86	0.55	799	86	0.82	0.030
Fuel 6	260	1.08	0.04	6.74	0.56	806	86	0.93	0.035
Fuel 7	255	1.29	0.12	4.29	0.64	802	83	1.21	0.242
Fuel 8	265	1.25	0.10	6.04	0.64	834	82	1.04	0.169
Fuel 9	261	1.29	0.09	5.07	0.50	824	83	2.14	0.143
Fuel 10	238	1.21	0.04	5.61	0.55	742	91	0.94	0.042
Fuel 11	235	1.31	0.13	4.22	0.58	733	89	1.09	0.231
Fuel 12	257	1.27	0.11	8.07	0.62	814	84	1.15	0.254
Fuel 13	242	1.50	0.12	1.39	0.26	761	85	1.09	0.492

549

EP 2 : 2280 rpm - 8.2 bar									
Fuel reference	BSFC (g/kWh)	NOx (g/kWh)	PM (g/kWh)	CO (g/kWh)	HC (g/kWh)	CO2 (g/kWh)	noise dB	stab %	C PM g/kWh
Fuel 1	279	1.15	0.15	3.72	0.18	876	90	0.69	0.123
Fuel 2	272	1.02	0.10	3.10	0.18	852	91	0.68	0.081
Fuel 3	283	1.06	0.20	4.05	0.17	891	89	0.74	0.109
Fuel 4	277	1.25	0.11	2.37	0.15	872	89	0.67	0.123
Fuel 5	253	1.26	0.19	1.73	0.26	792	88	0.69	0.143
Fuel 6	253	1.25	0.20	1.68	0.27	793	89	1.08	0.135
Fuel 7	257	1.30	0.21	1.57	0.30	811	88	0.65	0.209
Fuel 8	257	1.39	0.21	2.09	0.28	815	90	0.90	0.284
Fuel 9	258	1.52	0.20	1.30	0.24	822	88	0.90	0.276
Fuel 10	251	1.24	0.20	1.96	0.25	790	87	0.74	0.142
Fuel 11	246	1.18	0.18	1.62	0.20	774	88	1.17	0.149
Fuel 12	254	2.04	0.17	1.12	0.33	816	86	0.60	0.687
Fuel 13	258	1.27	0.22	1.79	0.20	812	87	0.62	0.223

550

551 *Appendix D: Synthesis of the models data of main engine outputs. Modeling was made on optimum*
 552 *results of EP1 (1500rpm – 6 bar) and EP2 (2280 rpm-8.2 bar): Correlation coefficients, standard*
 553 *deviations and determination coefficients*

Refinery stream	EP 1: 1500 rpm - 6 bar						
	BSFC	NOx	PM	CO	HC	Noise	Stability
	g/kWh	g/kWh	g/kWh	g/kWh	g/kWh	dB	%
HSRG	238	0.77	-0.03	6.41	0.48	89	0.46
HFCC	192	1.17	0.07	4.52	0.50	98	0.73
REF	228	0.96	0.11	12.71	0.68	85	1.95
HSRK	269	1.44	0.09	2.98	0.51	81	0.49
HCKK	263	1.50	0.10	2.23	0.43	80	1.66
HSRD	277	1.35	0.08	4.72	0.68	83	1.74
HCKLD	280	1.37	0.12	5.25	0.60	82	0.87
std dev	3.24	0.09	0.03	1.28	0.06	1.25	0.36
R ²	0.97	0.78	0.62	0.64	0.54	0.93	0.68

554

Refinery stream	EP 2: 2280 rpm - 8.2 bar						
	BSFC	NOx	PM	CO	HC	Noise	Stability
	g/kWh	g/kWh	g/kWh	g/kWh	g/kWh	dB	%
HSRG	223	1.4	0.3	-0.1	0.4	88	1.1
HFCC	213	1.3	0.3	-0.1	0.3	86	1.2
REF	207	3.3	0.3	-3.0	0.6	81	0.8
HSRK	262	0.9	0.1	2.9	0.2	93	0.9
HCKK	269	1.1	0.2	2.7	0.2	90	0.9
HSRD	279	1.2	0.1	2.8	0.2	89	0.7
HCKLD	286	1.0	0.1	4.1	0.1	89	0.6
std dev	3.03	0.10	0.04	0.55	0.03	0.33	0.22
R ²	0.97	0.93	0.45	0.84	0.90	0.97	0.31

555